# Mills FC, Johnson ML, Ackers GKOxygenation-linked subunit interactions in human hemoglobin: experimental studies on the concentration dependence of oxygenation curves. Biochemistry...

**ARTICLE** *in* BIOCHEMISTRY · DECEMBER 1976

Impact Factor: 3.02 · DOI: 10.1021/bi00669a023 · Source: PubMed

# Oxygenation-Linked Subunit Interactions in Human Hemoglobin: Experimental Studies on the Concentration Dependence of Oxygenation Curves†

Frederick C. Mills, Michael L. Johnson,‡ and Gary K. Ackers*

ABSTRACT: An experimental study on the concentration dependence of oxygenation curves for human hemoglobin has been carried out between $4 \times 10^{-8}$ M heme and $5 \times 10^{-4}$ M heme in 0.1 M tris(hydroxymethyl)aminomethane hydrochloride, 0.1 M NaCl, 1 mM disodium ethylenediaminetetraacetic acid, pH 7.4, 21.5 °C. With decreasing hemoglobin concentration the curves show pronounced shifts in position and shape, consistent with dissociation of tetrameric hemoglobin into dimeric species of high affinity and low cooperativity. Combination of these data with independently determined values of dissociation constants for unliganded and fully liganded hemoglobin permits a resolution of the seven parameters necessary to define the linked binding and subunit association processes. The total oxygenation-linked subunit dissociation energy (6.34 kcal) was resolved into intersubunit contact energy changes between $\alpha\beta$ dimers in tetrameric hemoglobin which accompany binding of the first, middle two, and last oxygen molecules. The resolution is accurate to within approximately ±0.3 kcal. To within this limit the isolated dimers are found to bind oxygen noncooperatively and with the same affinity as isolated $\alpha$ and $\beta$ chains. Equally good fits to the data are obtained when dimers are slightly anticooperative. At least three major energetic states are apparently assumed by hemoglobin tetramers, with respect to the $\alpha^1\beta^2$ contact region, corresponding to (a) unliganded, (b) singly liganded, (c) triply and quadruply liganded species. The results do not establish whether these states may be assumed by a single molecule, or whether they arise as averages over a distribution of conformational states. They do provide unequivocal evidence against a concerted transition at any particular binding step in a system with only two energetic states of tetramer (i.e., an all or none switchover between T and R states at a particular binding step).

Formulation of a detailed mechanism for hemoglobin action must ultimately depend upon establishing correlations between structural and energetic transitions which accompany the successive oxygen binding steps. At the present time there exists little information in either of these areas compared with what will eventually be required to establish a definitive theory for the mechanism of cooperativity and regulation in human hemoglobin. Knowledge of the thermodynamic states assumed by the tetrameric molecule during the cycle of oxygenation–deoxygenation is of particular importance since the very concept of cooperativity (i.e., change in binding free energy with degree of ligation) is a thermodynamic one. Detailed thermodynamic information provides a necessary guide to assessing mechanistic relevance of structural data since appreciable rearrangements in atomic coordinates may be accompanied by only minor net free energy transitions and vice versa (cf. Lumry, 1971; Weber, 1975).

Cooperative interactions between remote ligand binding sites in tetrameric human hemoglobin must be transmitted across contact regions[1] separating the subunits containing such sites. Studies on the kinetics and thermodynamics of dissociation processes affecting those contact regions may therefore provide information on the nature and energetics of the subunit interactions involved. Of particular interest is the determination of changes in intersubunit contact energy[2] and the corresponding changes in energy for binding ligand at each successive step. By comparing these quantities it is possible to establish what fraction of the cooperative energy is reflected at each step within the intersubunit contact region. Fundamental thermodynamic characterization of this type provides important constraints which must be met by any models purporting to explain the mechanism of action of hemoglobin.

The contact region of primary interest in the present study is that separating $\alpha^1\beta^1$ and $\alpha^2\beta^2$ dimer pairs within the tetramer. It is this contact plane where the major changes in quaternary structure are inferred from x-ray analysis to occur upon oxygenation (Perutz, 1970; Perutz and Ten Eyck, 1971). This is also the contact plane where noncovalent bonding interactions are destroyed upon dissociation of the tetramer into dimeric species in dilute solution near neutral pH (Rosemeyer and Huehns, 1967; Soni, 1973; Hewitt et al., 1972). Determining the energetics of hemoglobins with specific structural

† From the Department of Biochemistry, University of Virginia, Charlottesville, Virginia 22901. *Received April 26, 1976.* Supported by National Science Foundation Grant BMS 74-24507 and United States Public Health Service Grant GM-14493.

‡ Recipient of United States Public Health Service Postdoctoral Fellowship AM03201.

[1] It is recognized here that the intersubunit "communication" may be direct, or may be mediated indirectly through shifts in distributions of preexisting conformational states.

[2] The term "contact energy" will be used here to denote the bonding strength between a specified pair of subunits (each subunit may be a combination of polypeptide chains, e.g., an $\alpha\beta$ dimer). Operationally it equals the free energy for dissociation of the complex into its constituent subunit species. A bond of this type will in general arise from a combination of many microscopic interactions within the region of contact between the subunits, and will also contain contributions attributable to solvent interactions. These microscopic contributions to the bond may change in strength, number, or kind, in response to conformational perturbations associated with changes in environmental conditions, or with ligand binding at sites remote from the region of contact between subunits. It is these changes that we are interested in measuring. The term "contact energy" is thus a useful term for grouping energies of intersubunit interaction which contribute to the strength of association between subunit pairs.

modifications within this contact region may permit identification of pairwise interactions with cooperative events. Figure 1 shows the relationships between subunit dissociation and oxygen binding. The oxygenation-linked free energy of dissociating tetramers into dimers ($^4\Delta G_2 - {}^0\Delta G_2$, Figure 1) has been known for several years to be substantial, i.e., on the order of 6–8 kcal (Kellett, 1971b; Thomas and Edelstein, 1972, 1973). Recently we have succeeded in determining a value of 6.34 ± 0.2 kcal for this free energy coupling[3] under one set of conditions, from independent estimates of the dissociation constants for unliganded and fully oxygenated hemoglobin (Ip et al., 1976). In this paper we are concerned with the problem of how the oxygenation-linked free energy is partitioned with respect to the successive binding steps.

We report here a study of oxygenation curves determined as a function of hemoglobin concentration. The object of these experiments was to obtain saturation data representing the linkage function (Ackers and Halvorson, 1974):

$$\bar{Y} = \frac{[Z_2' + Z_4'(\sqrt{Z_2^2 + 4{}^0K_2Z_4[P_t]} - Z_2)]/4Z_4}{Z_2 + \sqrt{Z_2^2 + 4{}^0K_2Z_4[P_t]}} \quad (1)$$

where $Z_2$ and $Z_2'$ are functions of the binding constants to dimer and the oxygen concentration [X], and $Z_4$ and $Z_4'$ are corresponding functions of the tetrameric binding constants (see Appendix for exact definitions). Equation 1 also defines the relationship between oxygenation state $\bar{Y}$ and the hemoglobin concentration $[P_t]$.

Using this linkage function, the oxygenation data obtained in this study have been analyzed, in combination with independently determined free energies for dissociation of oxy- and deoxyhemoglobin, to estimate the free energies for dissociating tetramers into dimers in successive stages of ligation. The results also provide a determination of the sequential oxygen binding energies for dimeric and tetrameric species. Knowledge of all these quantities permits a calculation of the changes in intersubunit contact energy within the tetramer upon binding of the first, middle two, and last oxygen molecules (Ackers and Halvorson, 1974). These differences ($\delta\Delta G$'s) may be written:[4]

$$\delta\Delta G_{01} \equiv {}^1\Delta G_2 - {}^0\Delta G_2 = \Delta G_{41} - \Delta G_{21} \quad (2)$$

$$\delta\Delta G_{13} \equiv {}^3\Delta G_2 - {}^1\Delta G_2 = \Delta G_{42} + \Delta G_{43} - (\Delta G_{21} + \Delta G_{22}) \quad (3)$$

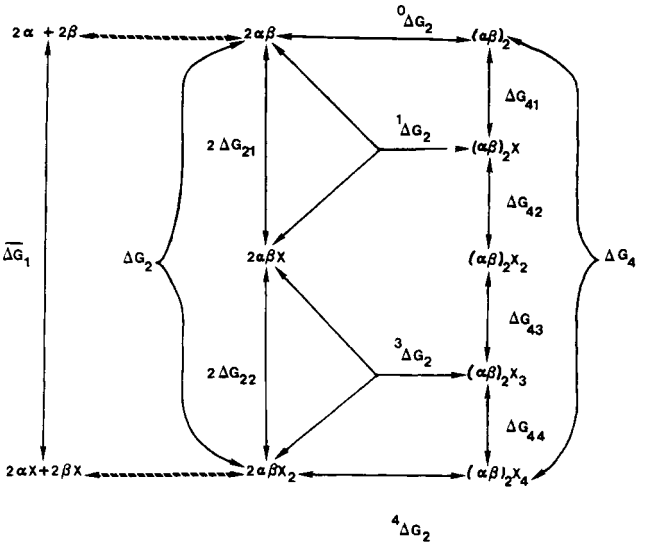


FIGURE 1: Linkage diagram for subunit dissociation and oxygenation of human hemoglobin. The energetic quantities represented have been defined previously (Ackers and Halvorson, 1974). $^0\Delta G_2$ and $^4\Delta G_2$ are free energies for tetramer formation (from dimers) in the unliganded and fully liganded states, respectively. $^1\Delta G_2$ and $^3\Delta G_2$ are respective association energies for formation of singly liganded tetramers (from combination of singly liganded and unliganded dimers) and triply liganded tetramers (from combination of singly and doubly liganded dimers). Energies for the successive binding steps to tetramer are $\Delta G_{41}$, $\Delta G_{42}$, $\Delta G_{43}$, $\Delta G_{44}$. For dimer, the successive free energies of oxygenation are $\Delta G_{21}$ and $\Delta G_{22}$. The free energies for saturation of tetramer and dimer, respectively, are $\Delta G_4$ and $\Delta G_2$. The successive differences ($^1\Delta G_2 - {}^0\Delta G_2$), ($^3\Delta G_2 - {}^1\Delta G_2$), and ($^4\Delta G_2 - {}^3\Delta G_2$) are measures of the intersubunit contact energy changes accompanying the first, middle two, and last binding steps, respectively. $\Delta G_1$ is the average free energy for oxygenating 2 mol of $\alpha$ chains and 2 mol of $\beta$ chains.

$$\delta\Delta G_{34} \equiv {}^4\Delta G_2 - {}^3\Delta G_2 = \Delta G_{44} - \Delta G_{22} \quad (4)$$

The approach we have used differs entirely from that of previous oxygenation studies which have been aimed at determining the tetrameric binding constants. Our primary focus of interest is upon the changes in dimer–dimer contact energy within tetrameric hemoglobin which accompany the successive binding steps. Although these are calculable from knowledge of the six binding constants to tetrameric and dimeric species and any one of the subunit association constants (e.g., that of unliganded hemoglobin), we have analyzed our data directly for the differences in dissociation energies. It should be noted that dimer binding isotherms for human hemoglobin A near neutral pH have never been determined and are not directly measurable by any known methods. Kinetic indicators (Anderson et al., 1971; Kellett, 1971a,b) suggest that dimer cooperativity may be very low, but do not permit quantitative estimation of the limits for such noncooperativity. Since the relationships between energetic quantities are of primary interest rather than their absolute values, we have felt it necessary to carry out as complete a determination as possible of the energies depicted in Figure 1. Equilibrium constants for all reactions denoted by the solid lines in this linkage scheme have been determined under the same conditions, so that accurate comparisons can be made. In a preliminary note (Ackers et al., 1976), we have summarized some of the principal results. Here we present a detailed description of the oxygenation studies. Methods and results of numerical analyses necessary to the interpretation of these experimental results are described in the following paper (Johnson et al., 1976).

[3] Free energies for dimer–tetramer association reactions determined in this study are based upon a reference state of 1 mol of dimer per l. at 21.5 °C and are not corrected to unitary values. Conversion to a molar heme basis requires adding $RT$ ln 2 to the association free energies. Differences between subunit association energies (e.g., $^4\Delta G_2 - {}^0\Delta G_2$) are of course independent of the concentration units, and expressed simply in kilocalories. The reference state for oxygen binding reactions in this study is 1 mol of dissolved $O_2$ per l., also at 21.5 °C. Oxygen concentrations in the experimental solutions were calculated from the measured oxygen tensions and the Henry's law constant: $1.77 \times 10^{-6}$ mol of $O_2$/mmHg.

[4] It is possible to separate the total free energy change $\delta\Delta G_{13}$ for the two middle binding steps in terms of an apparent free energy $^2\Delta G_2$ for formation of doubly liganded tetramer: $^2\Delta G_2 - {}^1\Delta G_2 = \Delta G_{42} - \Delta G_{22}$; $^3\Delta G_2 - {}^2\Delta G_2 = \Delta G_{43} - \Delta G_{21}$. However, the quantity $^2\Delta G_2$ is a combination of the formation free energies for the two kinds of doubly liganded tetramer that may be formed with respect to the contact region of interest. It equals $^2\Delta G_2{}^\Lambda - RT$ ln $(1 + K_1)$, where $^2\Delta G_2{}^\Lambda$ is the free energy for forming the "asymmetric" tetramer (i.e., with both ligands on an $\alpha^1\beta^1$ dimer) and $K_1$ is the constant defining the distribution between this species and the "symmetric" doubly liganded tetramer (i.e., with one ligand on each side of the $\alpha^1\beta^2$ contact region). The quantity $\delta\Delta G_{13}$ is rigorously equal to the change in bonding strength between dimers in going from the singly liganded to triply liganded states.

TABLE I: Enzyme Reduction System Used in Oxygenation Experiments.[a]

| Component | Concn of Stock: Molar | Concn of Stock: Working Unit Concn | Source and Type | ml Used per 5 ml of Hemoglobin Sample | Concn in Hemoglobin Sample: Molar | Concn in Hemoglobin Sample: Working Unit Concn |
|---|---|---|---|---|---|---|
| Glucose 6-phosphate | $5 \times 10^{-2}$ | 16.1 mg/ml | Calbiochem or Sigma | 0.1 | $1 \times 10^{-3}$ | 0.32 mg/ml |
| Glucose-6-phosphate dehydrogenase[b] | $4 \times 10^{-6}$ | 200 IU/ml | Calbiochem yeast lyophilized, grade A | These two components were stored together; 0.02 ml of this solution was used | $1.6 \times 10^{-6}$ | 0.81 unit/ml |
| NADP | $1.2 \times 10^{-2}$ | 10 mg/ml | Sigma | | $4.8 \times 10^{-5}$ | 0.04 mg/ml |
| Ferredoxin | $8.6\text{-}17.2 \times 10^{-5}$ | 1-2 mg/ml | Sigma, type III | 0.02 | $3.4\text{-}7.8 \times 10^{-7}$ | 4-8 μg/ml |
| Ferredoxin NADP reductase[b] | $1.5 \times 10^{-5}$ | 2 units/ml | Sigma from spinach lyophilized | 0.02 | $6 \times 10^{-8}$ | 0.064 unit/ml |
| Catalase | $8 \times 10^{-5}$ | $1 \times 10^{6}$ IU/ml | Calbiochem | 0.002 | $3.2 \times 10^{-8}$ | 4000 IU/ml |

[a] Based on the enzyme reduction system described by Hayashi et al. (1973). [b] These components were apparently inactivated when stored with EDTA. Therefore they were stored in EDTA-free buffer.

TABLE II: $P_{50}$'s for Deoxygenation and Reoxygenation Curves.

| Hemoglobin Concn (M Heme) | Wavelength, λ (nm) | $P_{50}$ Deoxy (mmHg) | $P_{50}$ Reoxy (mmHg) | % Met[a] |
|---|---|---|---|---|
| $3.82 \times 10^{-4}$ | 610 | 4.99 | 4.78 | 1.5 |
| $7.65 \times 10^{-5}$ | 480 | 4.81 | 4.66 | 0.5 |
| $7.65 \times 10^{-5}$ | 610 | 4.82 | 4.72 | 0.5 |
| $3.82 \times 10^{-5}$ | 563 | 4.80 | 4.62 | 0.02 |
| $5.4 \times 10^{-6}$ | 415 | 4.35 | 4.18 | 0.02 |
| $2.7 \times 10^{-7}$ | 415 | 2.85 | 2.45 | 3 |
| $8 \times 10^{-8}$ | 415 | 2.35 | 2.45 | 8 |
| $4 \times 10^{-8}$ | 415 | 2.00 | 1.35 | 11 |
| $4 \times 10^{-8}$ | 415 | 1.95 | | 11 |

[a] The amount of oxidation occurring during deoxygenation of the sample as determined from spectral scans. The amount of methemoglobin initially present before deoxygenation was less than 0.5% for the highest five concentrations and less than 1% for the others.

## Experimental Section

### *Materials*

*Hemoglobin Preparations.* Hemoglobin was prepared from the blood of a nonsmoker by the method of Williams and Tsay (1973). This method purifies the major $A_0$ component of hemoglobin, and also removes organic phosphates. Immediately after preparation, the hemoglobin was frozen in small droplets in liquid $N_2$ and stored in liquid $N_2$ until use. This procedure eliminated previously observed deterioration in the quality of the hemoglobin which occurred upon prolonged storage in solution at 4 °C. A single preparation of hemoglobin was used for each complete series of concentration-dependent oxygenation curves.

The hemoglobin was found to migrate as a single band during electrophoresis on linear gradient polyacrylamide gel electrophoresis in tris borate EDTA[5] buffer, pH 8.4. The preparation was checked for organic phosphate by the method of Ames and Dubin (1960) and found to contain no phosphate to within a resolution of 5 phosphate molecules per 100 hemoglobin tetramers.

Isolated α and β chains were separated by the *p*-mercuribenzoate method of Bucci and Fronticelli (1965). The *p*-mercuribenzoate was removed by the method of Tyuma et al. (1966), with the modification that the β-mercaptoethanol was used for the PMB removal from both α and β chains. Complete reduction of the chains into their SH forms was verified by the method of Winterhalter and Colosimo (1971).

*Buffers.* The buffer used in all oxygenation experiments was 0.1 M Tris, 0.1 M NaCl, 1 mM $Na_2EDTA$, titrated to pH 7.4 with HCl. Trizma base and $Na_2EDTA$ were from Sigma. The NaCl and HCl were obtained from Fisher. Double-glass-distilled water was used to make up the buffer.

*Enzyme Reductase System.* An enzymatic reduction system (Hayashi et al., 1973) was used to minimize hemoglobin oxidation during the oxygenation experiments. Table I shows the composition of this system.

### *Instrumentation and Methods*

*Automatic Oxygenation System.* The course of deoxygenation and subsequent reoxygenation of hemoglobin solutions was followed spectrophotometrically while the change in oxygen tension was monitored with an oxygen electrode (Imai et al., 1970). An oxygenation cell similar to that of Imai was made of 18-2 grade 316 stainless steel.[6] Hemoglobin in this cell became oxidized at about the same rate (Table II) as in an oxygenation cell made entirely of glass.[7] However, a similar oxygenation cell made earlier of grade 304 stainless steel[8] caused so much oxidation of the hemoglobin that experiments were rendered impossible, even in the presence of the reductase system.

Using a Cary 118C spectrophotometer, changes in hemoglobin solutions were measured during the oxygenation experiments. The oxygenation cell was mounted in a thermostatable cell holder. The sample compartment was fitted with an aluminum tower, which allowed electrical lines, gas, and cooling lines to be attached to the oxygenation cell without light

[5] Abbreviations used: EDTA, ethylenediaminetetraacetic acid; PMB, *p*-mercuribenzoate; Tris, tris(hydroxymethyl)aminomethane.

[6] Composition (maximum percent by weight): C, 0.1; Mn, 2.0; Si, 1.0; Cr, 16-18; Ni, 10-14; Mo, 2-3; Fe, balance.

[7] Designed by Dr. Donald Atha, University of Texas (Austin).

[8] Composition (maximum percent by weight): C, 0.08; Mn, 2.0; Si, 1.0; Cr, 18-20; Ni, 8-11; Fe, balance.

leaks. The analogue absorbance output of the spectrophotometer was fed into the $Y$ axis of an Esterline-Angus 2417TB $X$-$Y$ recorder.

A Beckman 39065 oxygen electrode was used to monitor the oxygen tension of the hemoglobin sample. Thin Teflon membrane (10 $\mu$m) used with the electrode was a gift of Dr. W. B. Elliot, Department of Biochemistry, State University of New York, Buffalo. Polarization current was supplied by a 9-V battery and the voltage impressed across the electrode was adjusted to 0.8 V with a potentiometer. The current output of the electrode was amplified by a Keithley 150B microvolt ammeter and the voltage output of the amplifier was recorded on the $X$ axis of the recorder.

*Control of Temperature and Hydration.* Temperature control was accomplished by circulation of water from an external water bath (Neslab PBC-4) through the thermostating jacket of the oxygenation cell. The temperature of the hemoglobin solution within the cell was measured with a Digitex thermometer (United Systems Model 1501) and found to fluctuate less than 0.03 °C during the course of an experiment. To ensure that there was no change in the concentration of the protein solution during an experiment, gas used for deoxygenation and oxygenation was bubbled in succession through two thermostated hydrators before entering the oxygenation cell. The hydrators, oxygenation cell, and the spectrophotometer sample compartment were all connected to the same water bath.

*Performance Characteristics of the System.* Periodic checks were made on the performance of the Cary 118C spectrophotometer. Linearity of the instrument was tested by measuring the absorbances of weighed dilutions of a standard solution of dichromate (Haupt, 1952). The instrument was found to maintain linearity to within 0.005 absorbance unit up to an absorbance of 2.0. The drift in absorbance readings of the oxygenation system when the cell was filled with water or buffer was less than 0.0005 absorbance unit/h. The slit width was adjusted to give a 1-nm band-pass for all experiments.

Performance characteristics of the oxygen-measuring system were also determined. Linearity of the system was tested by equilibrating with several $O_2$–$N_2$ gas mixtures (Matheson) in succession and noting the pen position on the $X$ axis of the recorder. Taking the air point to be 155 mmHg, the deviations of points from linearity were found not to exceed ±0.2 apparent mmHg.

It was found that the pen on the $X$-$Y$ recorder always returned to the initial air point on the $X$ axis after an experiment, indicating a high degree of stability.

*Preparation of Samples for Oxygenation Experiments.* Before each experiment, a small quantity of frozen hemoglobin stock was thawed. The concentration of this stock solution was calculated from measured absorbance in the visible region of a $^1/_{100}$ volume dilution (Benesch et al., 1973). For the experiments reported in detail here, its value was 2.67 mM heme. Except for concentrations above $10^{-4}$ M heme, a portion of stock solution was diluted into the experimental buffer and the concentration of that sample calculated from the dilution factor. Since the stock solution was in a different buffer from the one used in these experiments, samples with concentration higher than $10^{-4}$ M heme were prepared by passing the hemoglobin stock solution through a G-25 column equilibrated with the experimental buffer, and then making the necessary dilution. The concentrations of these samples were determined by measuring their absorbances in a 0.1-cm path length cell in the visible region.

*Procedure for Oxygenation Experiments.* Five milliliters of sample was placed in the oxygenation cell. At least 15 min was allowed for equilibration of the system while the sample was being stirred and air was being flowed over its surface. The experiment was begun when the absorbance reading of the spectrophotometer and the output of the oxygen electrode reached constant values. Deoxygenation was begun by flowing $N_2$ gas over the surface of the sample. At protein concentrations below approximately $10^{-4}$ M (heme) it was necessary to mix an $O_2$–$N_2$ gas mixture with $N_2$ gas when the fractional saturation was in the range of 95 to 25% in order to slow the progress of the experiment. Otherwise reading of the $O_2$ electrode was observed to lag appreciably behind the true $pO_2$. Once the fractional saturation was below 25%, pure $N_2$ gas was flowed over the solution until the oxygen electrode gave a constant reading indicating complete deoxygenation of the sample. At high protein concentrations the release of oxygen from the hemoglobin solution was sufficiently slow that pure nitrogen could be used throughout the experiment. Pure $N_2$ gas was also used to deoxygenate the hemoglobin chains. Reoxygenation of samples at all protein concentrations was accomplished by mixing increasing amounts of an $O_2$–$N_2$ gas mixture with the $N_2$ until the fractional saturation reached approximately 95%. Further reoxygenation was then carried out with air. The time required for either deoxygenation or reoxygenation varied between 40 min and 2.5 h, the longer times being required for deoxygenation at the highest protein concentrations. The time course of oxygenation-reoxygenation was recorded using the time base for the strip chart recorder of the Cary 118C spectrophotometer. Spectra of the hemoglobin sample were recorded before and after each oxygenation or deoxygenation in order to assess the amount of methemoglobin formed and the overall reversibility.

Since the experiments were carried out over a protein concentration range of four orders of magnitude, it was necessary to use several different wavelengths to obtain workable full scale absorbance changes in going from oxygenated to deoxygenated samples. For all wavelengths used the slit width was adjusted to give a 1-nm band-pass.

*Digitization and Processing of Data.* Numerical values for the $X$ and $Y$ coordinates of each oxygenation curve were recorded manually at 30–50 points and punched on cards for computer processing. Calculations were performed on a CDC 6400 computer using methods described in the following paper (Johnson et al., 1976). Data for deoxygenation curves only were used in the analyses presented here, in order to minimize the effects of oxidation and protein denaturation.

In experiments carried out at hemoglobin concentrations below $10^{-6}$ M (heme) a small and approximately constant linear decrease in absorbance with time was observed on the portions of the time base recording prior to, and after the deoxygenation-reoxygenation sequence. A correction to each point of these lowest concentration deoxygenation curves was therefore made, based upon the observed "baseline" slope. No such variations were observed nor corrections needed for the experimental results at concentrations higher than $10^{-6}$ M.

*Determination of End Points.* The 100% saturation end point was determined for each curve by extrapolating a plot of absorbance vs. $1/pO_2$ to infinite oxygen tension. The zero percent saturation end point was taken to be the point where the pen ceased to move on the $X$ axis of the recorder when pure $N_2$ gas was flowed over the sample. This point corresponded closely with the $N_2$ end point established by calibration of the electrode.

*Additional Controls.* A series of studies were carried out to determine: (1) reproducibility of the data; (2) whether the

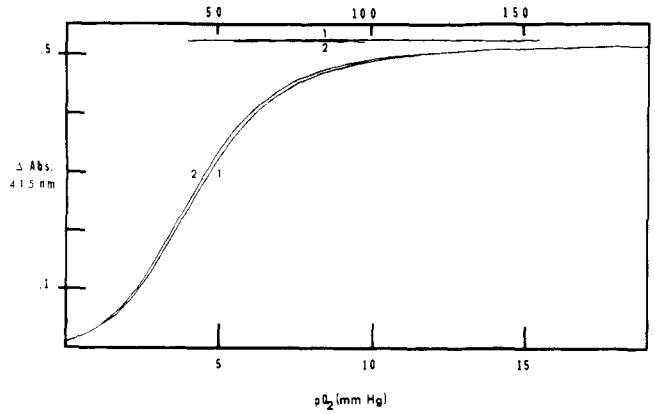


FIGURE 2: Oxygen binding curves at hemoglobin concentration of 5.4 $\times 10^{-6}$ M (heme) in 0.1 M Tris-HCl, 0.1 M NaCl, 1 mM $Na_2EDTA$, pH 7.4, 21.5 °C. (1) Deoxygenation curve; (2) reoxygenation curve. Experiments were carried out using the automatic oxygenation method of Imai with the methemoglobin reductase system of Hayashi.

enzyme reduction system appreciably perturbs the oxygenation curves; (3) whether the oxygenation curves are wavelength dependent under the conditions employed; and (4) whether differences in subunit association properties exist before and after an experiment, such as would arise from denaturation or irreversible dissociation to monomers (Kellett and Schachman, 1971). These tests were made by performing "large zone" gel chromatography experiments (cf. Ackers, 1975) before and after the deoxygenation-reoxygenation cycle.

## Results

*Oxygenation Curves.* Oxygenation-deoxygenation curves spanning a protein concentration range between $4.0 \times 10^{-8}$ and $3.82 \times 10^{-4}$ M (heme) were successfully measured. A typical pair of curves is shown in Figure 2 for a concentration of $5.4 \times 10^{-6}$ M. For solutions above $10^{-6}$ M heme, deoxygenation and reoxygenation curves were quite close (Figure 2) while for curves at lower concentrations, the separation became progressively greater.

Table II gives the $P_{50}$ values for the separate deoxygenation and reoxygenation curves as well as the amounts of oxidation at the end of each experiment. The closeness of the $P_{50}$ values for each pair of curves (their greatest separation generally being near the point of half-saturation) was taken as a measure of the reproducibility of the data (Imai, 1973). Curves were generally reproducible between separate experiments to within these same limits (Table II).

The enzyme reduction system was found not to alter detectably the $P_{50}$ values for the deoxygenation curves and was therefore deemed innocuous for the purposes of these experiments.

*Variation of Wavelength.* Four wavelengths were used to monitor the fractional saturation in these experiments: 610 and 480 nm for high concentrations ($3.82 \times 10^{-4}$, $7.65 \times 10^{-5}$ M heme), 563 nm for intermediate concentrations ($3.82 \times 10^{-5}$ M heme), and 415 nm for the low concentration curves ($5.4 \times 10^{-6}$, $4.0 \times 10^{-8}$ M heme). Plots of $Y$ axis pen deflection at one wavelength vs. $Y$ axis pen deflection at another wavelength for curves at the same concentration were highly linear. These results indicate that the oxygenation curves were independent of the wavelengths used to within limits of experimental precision (i.e., $\sim \pm 1\%$) in these buffer conditions.

*Concentration Dependence of Oxygenation Curves.* Data points from the deoxygenation curves are shown in Figures 3 and 4 as a function of hemoglobin concentration (Figures 3 and

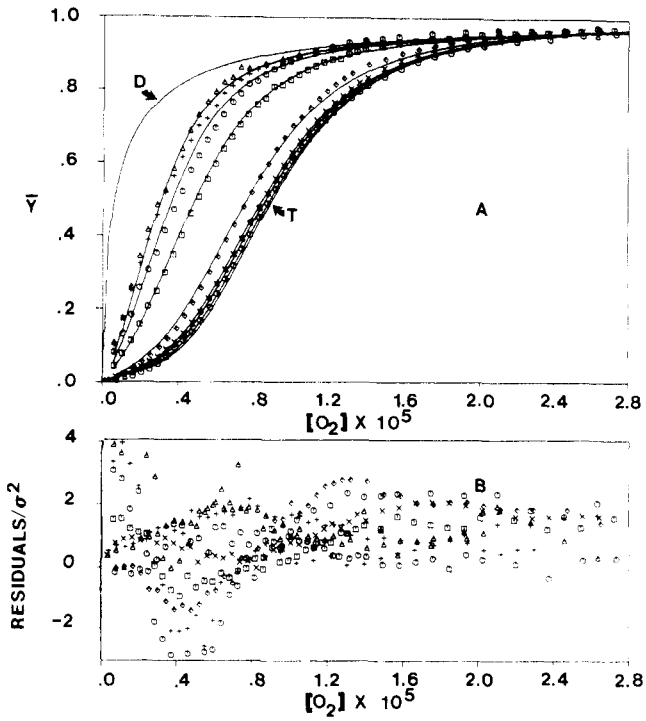


FIGURE 3: Oxygenation curves determined as a function of hemoglobin concentration and comparison between calculated curves (case A, Table V) and experimental data. (A) $\bar{Y}$ vs. $[O_2]$ as a function of hemoglobin concentration $[P_t]$. Each symbol type represents experimental data from an oxygenation curve measured at a given protein concentration and wavelength. The hemoglobin concentrations are the same as those given in Table II and decrease from right to left. The solid lines are the calculated curves for case A (Table V) at the experimental protein concentrations. Curves D and T are for dimer and tetramer, respectively. (B) Residuals of the best fit for all curves at various hemoglobin concentrations. The residuals were normalized to the variance of the fit, which was $1.01 \times 10^{-4}$. This fit yields slightly anticooperative oxygen binding by $\alpha\beta$ dimers.

4 show the same data points compared with different sets of solid curves, to be described below). It can be seen that pronounced changes in both shape and position occur as the hemoglobin is progressively diluted. The experimental curves bear a striking qualitative resemblance to the behavior predicted earlier for a linked dimer-tetramer system (Ackers and Halvorson, 1974).

*Standard Indicators of Hemoglobin Function.* Table III shows the values of $P_{50}$, median ligand concentration $[\overline{X}]$, Hill coefficient $n_{max}$, and Wyman free energy of interaction $\Delta G_I$ at each protein concentration. The asymptotic limbs for Hill plots in a dimer-tetramer system are calculated from the following limiting forms (see Appendix for derivation):

$$\left(\frac{\bar{Y}}{1-\bar{Y}}\right)_{[X]\to 0} = \frac{4K_{21} + K_{41}(\sqrt{1+4^0K_2[P_t]}-1)[X]}{4(1+\sqrt{1+4^0K_2[P_t]})} \quad (5)$$

$$\left(\frac{\bar{Y}}{1-\bar{Y}}\right)_{[X]\to\infty} = \frac{4K_{44}(K_{22}+\sqrt{K_{22}^2+4^0K_2[P_t]K_{44}})[X]}{4K_{44}K_{21}+K_{43}(\sqrt{K_{22}^2+4^0K_2[P_t]K_{44}}-K_{22})} \quad (6)$$

The Wyman interaction energy $\Delta G_I$ (Wyman, 1964) is calculated from these asymptotes as:

$$\Delta G_I = RT\left[\ln\left(\frac{\bar{Y}}{1-\bar{Y}}\right)_{[X]\to 0} - \ln\left(\frac{\bar{Y}}{1-\bar{Y}}\right)_{[X]\to\infty}\right] \quad (7)$$

The quantity $\Delta G_I$ is seen to vary with protein concentration $[P_t]$ and to contain information on all of the equilibrium con-

TABLE III: Standard Indicators of Hemoglobin Function.

| Protein Concn (M Heme) | $P_{50}$ (mmHg) | Median $O_2$ Pressure,[a] $X_{med}$ (mmHg) | Hill Coeff, $n_{max}$ | Wyman[b] Interaction Energy, $\Delta G_I$ (kcal) |
|---|---|---|---|---|
| $3.82 \times 10^{-4}$ | 4.99 | 4.89 | 3.28 | 2.79 |
| $7.65 \times 10^{-5}$ | 4.82 | 4.61 | 3.20 | 2.77 |
| $3.82 \times 10^{-5}$ | 4.80 | 4.52 | 3.32 | 2.76 |
| $5.36 \times 10^{-6}$ | 4.35 | 4.14 | 3.23 | 2.71 |
| $2.7 \times 10^{-7}$ | 2.85 | 2.70 | 2.48 | 2.42 |
| $8 \times 10^{-8}$ | 2.35 | 2.07 | 2.40 | 2.21 |
| $4 \times 10^{-8}$ | 2.00 | 1.72 | 2.21 | 2.06 |

[a] These values were converted into median oxygen concentrations $[\bar{X}]$ using the Henry's law constant: $1.77 \times 10^{-6}$ mol of $O_2$/mmHg. [b] The value of $\Delta G_I$ for tetrameric hemoglobin was determined in this study to be −2.8 kcal.

stants of the system. In practice its evaluation from experimental data is subject to large error and it does not provide a useful transformation of the linkage function eq 1 for estimation of parameters. In fact, the values of $\Delta G_I$ listed in Table III were obtained by the reverse procedure: we first evaluated all the equilibrium constants (described below) and then calculated $\Delta G_I$ analytically using eq 5 and 6.

The Hill coefficient for tetramer under these experimental conditions is near 3.3, probably reflecting the influence of EDTA and chloride anions which are present in molar excess in the system. The EDTA is used to minimize oxidation and irreversible dissociation into chains (Kellett and Schachman, 1971; Rifkind, 1974). It also appears to exert some of the effects of DPG and other organic polyanions such as those studied by Shimizu and Bucci (1974). We have found that the presence of 1 mM EDTA shifts the $P_{50}$ for a hemoglobin solution ($2.5 \times 10^{-5}$ M heme) from 3.75 to 4.75 mmHg under present experimental conditions.

## Analysis of the Oxygenation Data

The principal aim of our analysis was to determine the differences in subunit dissociation energies for tetrameric species corresponding to changes in state of ligation. We proceeded toward this goal by first determining independently some of the parameters necessary to define the linkage system (Figure 1) and then estimating the remaining ones by least-squares analysis of the oxygenation data. The reader should refer to the following paper (Johnson et al., 1976) for definitions of terminology, a description of the numerical methods used, and an assessment of their reliability for this problem.

*Calculation of the Free Energies for Totally Oxygenating Tetramers, Dimers, and Monomers.* The equilibrium constant $K_{44}$ for binding four oxygens to the tetramer was calculated from the median ligand concentration $[\bar{X}]$ of each oxygenation curve according to the formula (see accompanying paper for derivation):

$$K_{44} = [\bar{X}]^{-4}\left\{\frac{1 - {}^4f_2}{1 - {}^0f_2}\right\} \exp({}^0f_2 - {}^4f_2) \qquad (8)$$

where

$${}^4f_2 = \frac{(1 + 4{}^4K_2[P_t])^{1/2} - 1}{2{}^4K_2[P_t]}, \quad {}^0f_2 = \frac{(1 + 4{}^0K_2[P_t]^{1/2} - 1}{2{}^0K_2[P_t]}$$

The dimer–tetramer association constants $^0K_2$ and $^4K_2$ for unliganded and fully oxygenated hemoglobin, respectively,

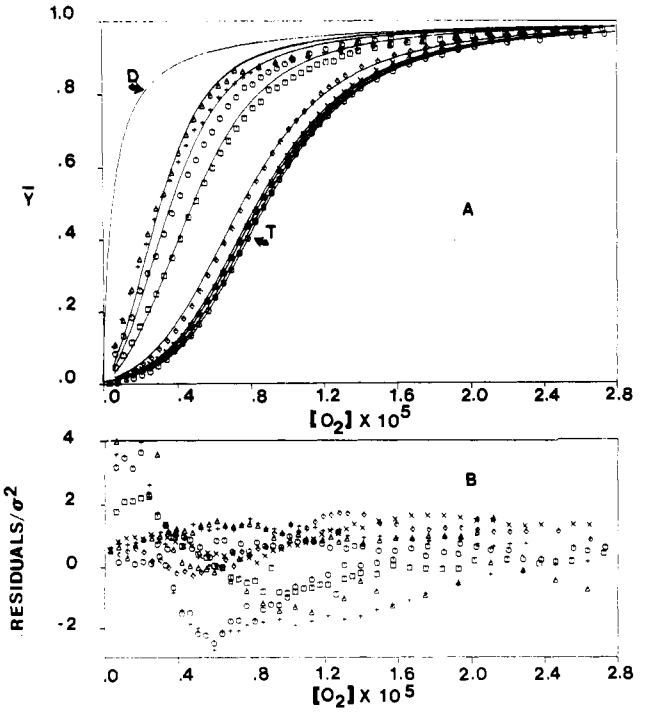


FIGURE 4: Analysis of concentration-dependent oxygenation curves in terms of case B (Table V) assuming noncooperative dimer. (A) Comparison between experimental data points and calculated curves (solid lines) from the best fit to the dimer–tetramer linkage scheme (Figure 1) assuming noncooperative dimer (case B, Table V). Curves D and T are for dimer and tetramer, respectively. (B) Residuals of the fit for all the data normalized to the variance of fit: $2.24 \times 10^{-4}$.

TABLE IV: Median Oxygen Concentration and Total Binding Energy.

| Hemoglobin Concn, $[P_t]$, (M Heme × $10^6$) | Median, $[\bar{X}]$ (M $O_2$ × $10^6$) | Calcd[a] $K_{44} \times 10^{20}$ ($M^{-4}$) |
|---|---|---|
| 382 | 8.67 | 1.60 |
| 76.5 | 8.21 | 1.76 |
| 76.5 | 8.16 | 1.80 |
| 38.2 | 8.01 | 1.78 |
| 5.4 | 7.32 | 1.60 |
| 0.27 | 4.78 | 1.53 |
| 0.08 | 3.67 | 1.53 |
| 0.04 | 3.05 | 1.68 |
| 0.04 | 3.17 | 1.44 |
| Mean Adair constant for four oxygens | | 1.64 ± 0.04 |
| $\Delta G = -27.16 \pm 0.05$ kcal/4 mol of $O_2$ | | |

[a] Calculated according to eq 4, using the independently determined values: $^0K_2 = 9.81 \times 10^5$ $M^{-1}$ (dimer). In these calculations, it is assumed that activity coefficients are near unity, so that the $[\bar{X}]$ does not differ appreciably from the median ligand activity.

were determined separately under conditions identical with those of the present study, and with hemoglobin samples prepared and handled in precisely the same manner (Ip et al., 1976). The values obtained were: $^0K_2 = 5.11 \times 10^{10}$ $M^{-1}$ (dimer), $^4K_2 = 9.81 \times 10^5$ $M^{-1}$ (dimer). Values of $K_{44}$ estimated for all the oxygenation curves, shown in Table IV, were found to be in good agreement. The average energy $\Delta G_4$ corresponding to these constants is $-27.16 \pm 0.05$ kcal/4 mol of $O_2$ bound. Estimation of this energy is independent of the de-

TABLE V: Detailed Analyses of Concentration-Dependent Oxygenation Data.

| | Case A | | Case B | | Case C | |
|---|---|---|---|---|---|---|
| | Value | Range | Value | Range | Value | Range |
| Fixed parameters | | | | | | |
| $^0K_2$ | $5.108 \times 10^{10}$ | *a* | $5.108 \times 10^{10}$ | *a* | $5.108 \times 10^{10}$ | *a* |
| $^4K_2$ | $9.810 \times 10^5$ | *a* | $9.810 \times 10^5$ | *a* | $9.810 \times 10^5$ | *a* |
| $K_{44}$ | $1.640 \times 10^{20}$ | *a* | $1.640 \times 10^{20}$ | *a* | $1.71 \times 10^{20}$ | *a* |
| $K_{22}$ | $2.922 \times 10^{12}$ | *a* | $2.922 \times 10^{12}$ | *a* | $2.98 \times 10^{12}$ | *a* |
| Estimated parameters | | | | | | |
| $^0K_2/^1K_2$ | 146.3 | (119.1, 205.3) | 71.67 | (57.28, 91.69) | 75.35 | (68.31, 81.37) |
| $^3K_2/^4K_2$ | 0.773 | (0.516, 1.080) | 1.737 | (1.008, 2.759) | 1.245 | (1.042, 1.527) |
| $K_{coop2}$ | 1.950 | (1.647, 2.187) | 1.000 | *c* | 1.000 | *c* |
| $\sqrt{k_{43}}$ | $-8.64 \times 10^{41}$ | $(-1.10 \times 10^{49}, 4.26 \times 10^{49})$ | $-4.50 \times 10^{14}$ | $(-2.02 \times 10^{22}, 1.62 \times 10^{22})$ | 651.5 | (385.8, 1361.0) |
| $K_{21}$ | $6.667 \times 10^6$ | *b* | $3.419 \times 10^6$ | *c* | $3.454 \times 10^6$ | *c* |
| $K_{41}$ | $4.557 \times 10^4$ | *b* | $4.770 \times 10^4$ | *b* | $4.583 \times 10^4$ | $(2.560 \times 10^4, 6.78 \times 10^4)$ |
| $K_{42}$ | $3.873 \times 10^{-70}$ | *b* | $2.427 \times 10^{-24}$ | *b* | $5.800 \times 10^8$ | $(-3.257 \times 10^9, 4.111 \times 10^9)$ |
| $K_{43}$ | $2.892 \times 10^{14}$ | *b* | $4.920 \times 10^5$ | *b* | $2.462 \times 10^{14}$ | $(-0.166 \times 10^{14}, 5.319 \times 10^{14})$ |
| $\delta\Delta G_{01}$ | 2.91 | (−2.79, −3.11) | 2.49 | (−2.36, −2.64) | 2.52 | (2.46, 2.57) |
| $\delta\Delta G_{13}$ | 3.58 | *b* | 3.35 | *b* | 3.69 | *b* |
| $\delta\Delta G_{34}$ | −0.15 | (−0.39, −0.04) | 0.32 | (0.01, 0.59) | 0.13 | (0.02, 0.25) |
| Variance of fit | | | | | | |
| | $1.01 \times 10^{-4}$ | | $2.24 \times 10^{-4}$ | | $2.25 \times 10^{-5}$ | |

[a] Evaluated independently (see text). [b] Derived quantities. Only fitted quantities have confidence ranges, corresponding to one standard deviation. [c] Values for assumed noncooperative dimer.

tailed shapes of oxygenation curves and is not highly correlated with the other energies necessary to describe the linkage system.

From the free energies $^0\Delta G_2$, $^4\Delta G_2$, and $\Delta G_4$ (corresponding to equilibrium constants $^0K_2$, $^4K_2$, and $K_{44}$), the energy for binding two oxygens to the dimer was calculated as:

$$\Delta G_2 = (\Delta G_4 + {}^0\Delta G_2 - {}^4\Delta G_2)/2 =$$

$$-16.75 \pm 0.25 \text{ kcal/2 mol of } O_2$$

The free energies for binding oxygen to isolated chains were determined by fitting each of their oxygenation curves to a rectangular hyperbola, giving $-8.20 \pm 0.05$ kcal/mol of $O_2$ for $\alpha$ chains and $-8.30 \pm 0.05$ kcal/mol of $O_2$ for the $\beta$ chains. These energies sum to $-16.5 \pm 0.1$ kcal/2 mol of $O_2$, in good agreement with $\Delta G_2$.

The difference between the oxy and deoxy subunit association free energies ($\delta\Delta G_{04}$) is $6.34 \pm 0.2$ kcal ($^0\Delta G_2 = -14.38$ kcal/mol of dimer, $^4\Delta G_2 = -8.05$ kcal/mol of dimer). This represents the total oxygenation-linked subunit contact energy, which must be partitioned into energy differences for the successive stages of ligation. Determination of this partitioning requires further analysis of the oxygenation data, including information contained in the shapes and positions of the saturation curves.

*Analysis of the Oxygenation Data for the Remaining Free Energies.* The oxygenation data were analyzed by least-squares minimization to the saturation function for a dimer–tetramer hemoglobin system (Ackers and Halvorson, 1974; Johnson et al., 1976). We initially fixed the values of $^0K_2$, $^4K_2$, and $K_{44}$ and estimated values for several different sets of the four remaining independent parameters. A useful parameter set for such analyses includes $K_{coop2}$, $^0K_2/^1K_2$, $^3K_2/^4K_2$, and $\sqrt{K_{43}}$[9] (see the following paper in this issue). From the seven parameters listed above, all energies associated with the dimer–tetramer linkage scheme may be calculated.

We first analyzed all of the oxygenation curves to obtain the best fit over the widest concentration range available. Results of this analysis are listed in Table V. The energy distribution estimated by this type of four parameter analysis is designated case A. The analysis yielded a slight negative cooperativity for the dimer oxygen binding and little or no difference between $^3K_2$ and $^4K_2$, corresponding to the last step of oxygen binding by tetramer. The fit of this energy distribution to the experimental data is illustrated in Figure 3.

The finding of small apparent anticooperativity in the dimer is suspect on the basis of (1) the near equality between $\Delta G_2$ and the summed oxygenation energies for the isolated chains, (2) previous kinetic indicators (Anderson et al., 1971; Kellett, 1971a,b), which strongly suggest dimer noncooperativity, (3) the findings of Hewitt et al. (1972) demonstrating noncooperativity in isolated dimers of des-Arg-141 hemoglobin. (4) An entirely independent set of oxygenation curves yielded results highly consistent with those of the data sets described in detail here, with the exception that the dimers had slight positive cooperativity. (5) It seems likely that small amounts of oxidation of one of the binding sites on some of the free dimers

[9] $^0K_2$, $^1K_2$, $^3K_2$, and $^4K_2$ are dimer–tetramer association constants for formation of unliganded, singly, triply, and quadruply liganded tetramers, respectively. $K_{coop2}$ is a parameter equal to $K_{21}/(2\sqrt{K_{22}})$ where $K_{21}$ and $K_{22}$ are product Adair constants for oxygen binding onto dimers. $k_{43}$ is the sequential constant for the third binding step to tetramers. For further discussion of the quantities used here, see the following paper (Johnson et al., 1976).

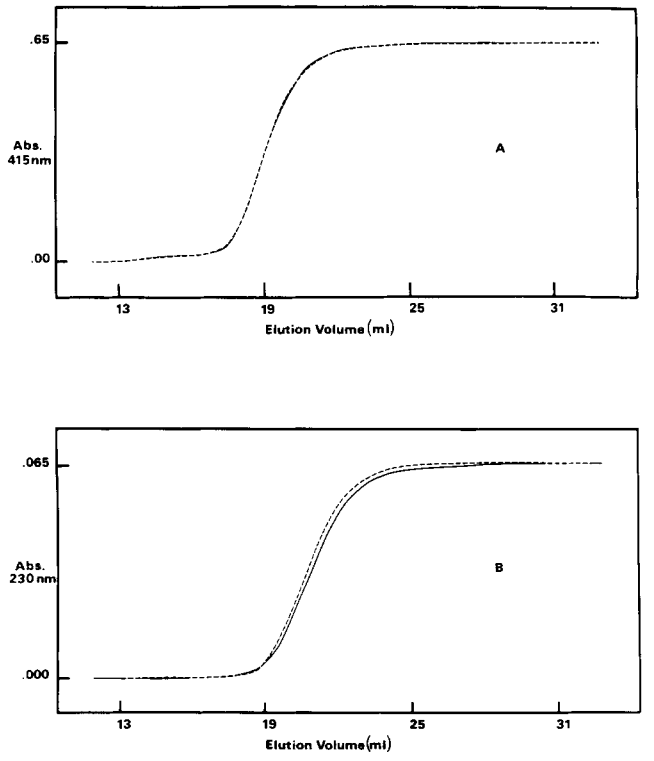


FIGURE 5: Leading boundaries of large zone gel chromatography experiments carried out on hemoglobin solutions before (dashed lines) and after (solid lines) oxygenation–deoxygenation. Hemoglobin concentrations were: (A) $5 \times 10^{-6}$ M (heme); (B) $5 \times 10^{-7}$ M (heme). Experiments were carried out with a Sephadex G-100 (Pharmacia) column, 1.5 × 40.0 cm, at 21.5 °C. Effluent was monitored with a Gilford spectrophotometer. The irreversibility shown in curve B results in shifts of centroid position from 19.36 to 19.50 ml in the elution profiles. No such irreversibility is observed at the higher concentration.

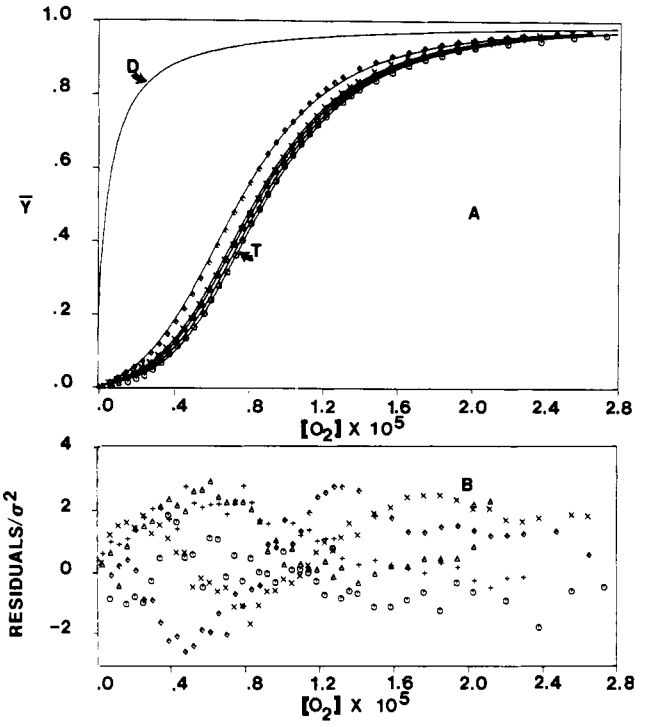


FIGURE 6: Analysis of oxygenation data for highest hemoglobin concentrations between 5.4 (heme) and 382 $\mu$M (heme). (A) Solid curves are calculated from best fit, case C (Table V). (B) Curves D and T are calculated binding isotherms for dimer and tetramer, respectively. Distribution of residuals normalized to the variance of the fit: $2.55 \times 10^{-5}$.

could produce an apparent negative dimer cooperativity by lowering the net concentration of second-oxygen binding sites. Therefore we explored the analysis using a fixed ratio between $K_{21}$ and $K_{22}$ so as to give a noncooperative dimer (i.e., $K_{coop2}$ was set equal to unity). We then fitted the oxygenation curves for only three remaining parameters ${}^0K_2/{}^1K_2$, ${}^3K_2/{}^4K_2$, and $\sqrt{K_{43}}$, having fixed the other four quantities necessary to define the system. This gave a best fit with a variance only slightly greater than that obtained when four parameters were floated. The resulting free energy distribution, designated case B, is shown in Table V and the fit to the data illustrated in Figure 5.

Based on extensive simulation and analyses of the fitting problem at hand (some of which is described in the following paper in this issue), both cases A and B are found to represent good fits to the experimental data. However, there are clearly systematic differences in both cases (Figures 3 and 4) between the experimental data points and curves calculated from the estimate of parameters from the composite of all data points. The possible sources of these deviations may be divided into three categories: (1) the basic linkage scheme is incorrect; (2) the linkage scheme is correct but the true minimum was not found in the least-squares calculations, so that a false estimate of the parameters was obtained; (3) there are systematic errors in the data. Although possibilities 1 and 2 cannot be ruled out categorically (see Discussion), there is ample reason to believe that most of the deviations are attributable to systematic errors in the data for the four lowest hemoglobin concentrations. These curves, below 1 $\mu$M heme, were associated with dramatically greater oxidation (Table II), required correction for apparent drift (as described in Methods), showed detectable alterations in their gel chromatography profiles (shown in Figure 5), and were generally subject to greater experimental uncertainty (e.g., denaturation and surface adsorption effects).

We therefore tried fitting simultaneously to the five data sets corresponding only to the highest concentrations, i.e., 5.4–382 $\mu$M. It should be noted that, in principle, a single oxygenation curve at sufficiently low hemoglobin concentration to encompass appreciable subunit dissociation could be analyzed to yield all of the energies. The effects of error levels on analyses of oxygenation curves are explored in the following paper (Johnson et al., 1976). Results of the best fit to the five highest concentration curves, designated case C, are shown in Table V and in Figure 6. It can be seen that the variance is lower by an order of magnitude as compared with case B, and the distribution of residuals (Figure 4) appears to be random.[10] It is shown in the following paper (Johnson et al., 1976) that the variance of fit obtained in case C is well within the limits for meaningful estimation of parameters when the errors are randomly distributed. It should also be noted that the energy distribution of case C is essentially the same as case B and, to within error limits, the same as case A. Estimation of $K_{42}$ and $K_{43}$ is subject to large uncertainty as expected (see Discussion). In general these cases serve to illustrate the limits of resolution

[10] Although the composite of all oxygenation curves appears essentially random, the successive data points for any single oxygenation curve will inevitably exhibit some correlation in deviations from the best fit, due to the manner in which the data are determined. Thus, even these data will not pass the most stringent tests for randomness. In experimental systems of this kind, values of the dependent variable must be collected using a random order in values of the independent variable in order to eliminate this problem.

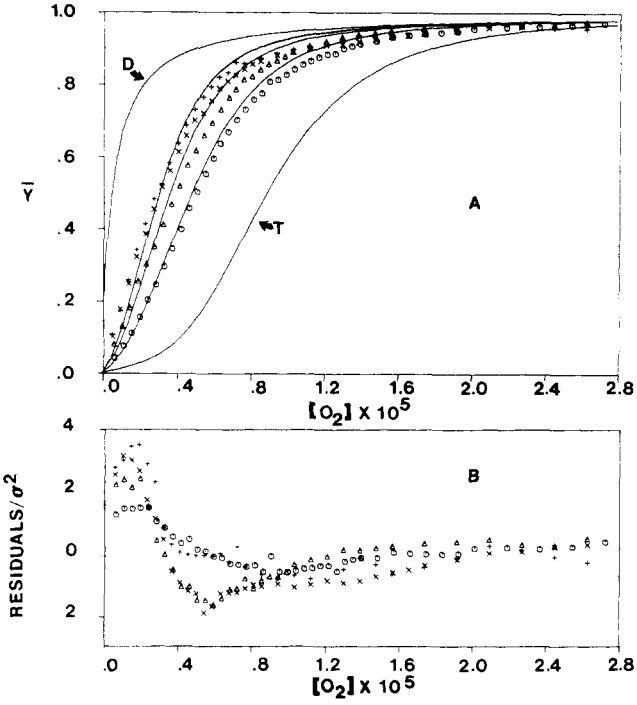


FIGURE 7: (A) Comparison between low concentration data points and case C analysis (Table V). Solid lines were calculated for the experimental concentrations and the derived case C energy distribution. Curves D and T are calculated isotherms for dimers and tetramers, respectively. (B) Distribution of residuals normalized to the variance: $8.2 \times 10^{-4}$.

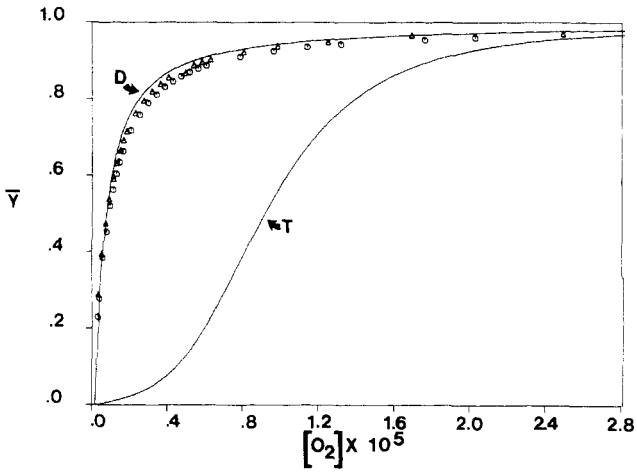


FIGURE 8: Comparison of oxygen binding data measured for $\alpha$ chains (○) and $\beta$ chains (△) with dimer binding isotherm (solid curve on left) calculated from independent estimates of ${}^0K_2$, ${}^4K_2$, and $K_{44}$, and assuming noncooperative dimer.

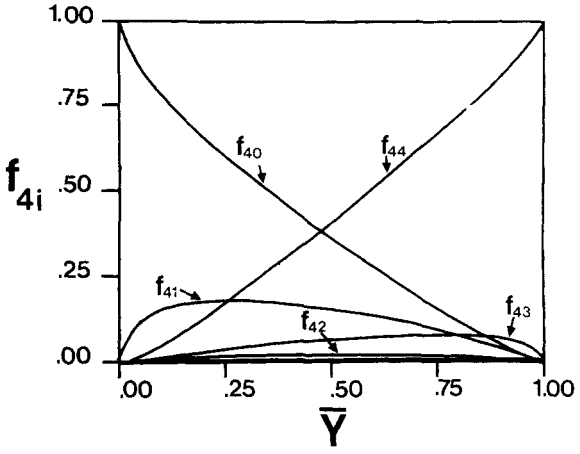


FIGURE 9: Relative abundance of tetrameric hemoglobin in various liganded states under conditions of this study. Distributions were calculated from the case C equilibrium constants and tetramer Adair equation.

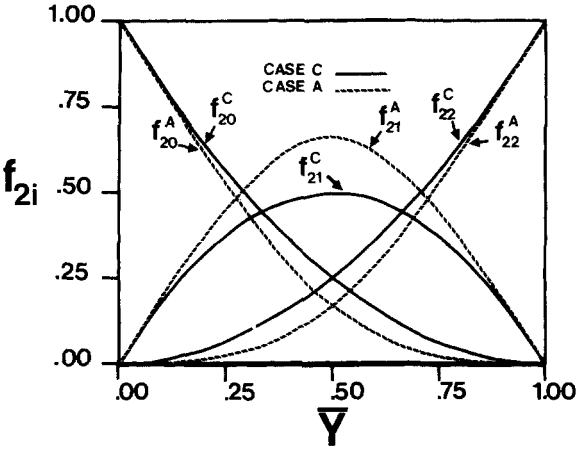


FIGURE 10: Relative abundance of dimeric species under conditions of this study. (—) Noncooperative dimer (case C results); (- - -) anticooperative dimer (case A results).

presently obtainable. We have found, by extensive further analyses and simulation, that a "tolerance" of approximately ±0.3 kcal can be accommodated nearly anywhere on the scheme (Figure 1) with approximately equally good fit to the data. We thus conclude that the energy distribution can be resolved only to within these limits, although we prefer the noncooperative dimer on the basis of arguments mentioned above. Analyses carried out using three entirely different sets of parameters (described in the following paper) were found to converge to the same energy distribution. An entirely independent set of oxygenation curves, covering a slightly narrower concentration range, yielded results highly consistent with those of the data sets described in detail here.

In Figure 7 the four lowest concentration data sets are compared with the oxygenation curves (solid lines) calculated from analysis of the highest concentration data, case C. It is seen that the general shapes and positions of the calculated and experimentally derived data at these lowest concentrations are in good agreement although systematic derivations in detailed shape are clearly evident as with cases A and B.

Comparison between the isolated chain data and the oxygenation curve for dimer corresponding to case C is shown in Figure 8. It can be seen that the agreement is close, with a slightly higher affinity for the dissociated dimers (solid curve). Figures 9 and 10 show the derived distribution of the successively liganded species of tetramer and dimer under conditions of this study. The fraction of hemoglobin present in the form of dimers as a function of saturation is shown in Figure 11 for the hemoglobin concentrations used in this study.

Table VI lists the derived free energies corresponding to the case C analysis for ligand binding by dimers and tetramers, and for subunit association. Values of these quantities after correction for statistical factors are also listed. It is these resulting intrinsic quantities, denoted by primed symbols $\Delta G'$, which are of greatest interest in assigning free energy changes to molecular events. For example, the Wyman interaction energy for tetramers (commonly taken as a fundamental measure of cooperativity) is calculated from values listed in the right hand column of Table VI: $\Delta G_{44}' - \Delta G_{41}' = 2.8$ kcal (Saroff and

TABLE VI: Free Energies of the Linkage System.

| | Macroscopic $\Delta G$ | Statistical Term[a] | Intrinsic $\Delta G'$ |
|---|---|---|---|
| | Subunit Association Energies | | |
| ${}^0\Delta G_2$ | −14.38 ± 0.2 | $RT$ ln 1 | −14.38 ± 0.2 |
| ${}^1\Delta G_2$ | −11.86 ± 0.3 | $RT$ ln 2 | −11.46 ± 0.3 |
| ${}^2\Delta G_2$ | −9.40 ± 0.3 | $RT$ ln 6 | −8.36 ± 0.3 |
| ${}^3\Delta G_2$ | −8.18 ± 0.25 | $RT$ ln 2 | −7.78 ± 0.25 |
| ${}^4\Delta G_2$ | −8.05 ± 0.2 | $RT$ ln 1 | −8.05 ± 0.2 |
| | Intersubunit Contact Energy Changes | | |
| $\delta\Delta G_{01}$ | 2.52 ± 0.30 | $RT$ ln ½ | 2.92 ± 0.30 |
| $\delta\Delta G_{12}$ | 2.46 ± 0.32 | $RT$ ln ⅓ | 3.10 ± 0.32 |
| $\delta\Delta G_{23}$ | 1.23 ± 0.32 | $RT$ ln 3 | 0.59 ± 0.32 |
| $\delta\Delta G_{34}$ | 0.13 ± 0.30 | $RT$ ln 2 | −0.27 ± 0.3 |
| | Binding Free Energies | | |
| $\Delta G_{21}$ | −8.78 ± 0.28 | $RT$ ln 2 | −8.38 ± 0.28 |
| $\Delta G_{22}$ | −7.97 ± 0.21 | $RT$ ln ½ | −8.38 ± 0.21 |
| $\Delta G_{41}$ | −6.26 ± 0.21 | $RT$ ln 4 | −5.45 ± 0.21 |
| $\Delta G_{42}$ | −5.51 ± 0.54 | $RT$ ln ⅔ | −5.28 ± 0.54 |
| $\Delta G_{43}$ | −7.56 ± 0.63 | $RT$ ln ⅔ | −7.80 ± 0.63 |
| $\Delta G_{44}$ | −7.85 ± 0.42 | $RT$ ln ¼ | −8.25 ± 0.42 |

[a] The statistical term when subtracted from the macroscopic free energy yields the intrinsic free energy.

Minton, 1972).

The apparent subunit association energy $\overline{{}^2\Delta G_2}$ corresponding to the formation of doubly liganded tetramer has also been listed in Table VI, although this quantity does not represent a simple average of the association energies for the two kinds of doubly liganded tetramer (see footnote 3). It is possible to make estimates based on the limits of $K_1$: if only one type of doubly liganded tetramer exists, then $\overline{{}^2\Delta G_2}$ will represent that species. If on the other hand a purely random distribution exists (i.e., equal intrinsic binding constants to form the two types of species), then $K_1$ will equal 4, and ${}^2\Delta G_2{}^S = {}^2\Delta G_2{}^A = -8.46$ kcal/mol of dimer.

*The Intersubunit Contact Energies.* Using the case C analysis the changes in intersubunit contact energy associated with the successive stages of oxygen binding by tetramers may be calculated. Based on the intrinsic subunit association energies (corrected for statistical factors), we have for the three stages of oxygenation:

$$\text{first step: } \delta\Delta G_{01}' = {}^1\Delta G_2' - {}^0\Delta G_2' = 2.92 \pm 0.3 \text{ kcal}$$

$$\text{middle steps: } \delta\Delta G_{13}' = {}^3\Delta G_2' - {}^1\Delta G_2' = 3.69 \pm 0.4 \text{ kcal}$$

$$\text{last step: } \delta\Delta G_{34}' = {}^4\Delta G_2' - \Delta G_2' = -0.27 \pm 0.3 \text{ kcal}$$

Thus the 6.34 kcal of oxygenation-linked subunit interaction energy is partitioned so that approximately 2.9 kcal of "constraining" energy is released within the contact region upon binding of the first oxygen, and approximately 3.7 kcal during the second and third binding steps. There appears to be no significant intersubunit contact energy change at the last binding step.

## Discussion

*The Automatic Oxygenation Technique.* From the results obtained in this study we have been able to confirm that the rapid automatic oxygenation method of Imai (Imai et al., 1970; Imai, 1973) does permit reproducible measurements of highly precise oxygenation curves under carefully controlled conditions. The present study provides new information on the limits of the technique for measurements at the lowest protein concentrations. At concentrations below approximately 1 $\mu$M heme, the quality of data obtained deteriorates appreciably by comparison with the highly precise (ca. ±0.5%) values obtainable at the higher concentrations. The limiting factors appear to be oxidation and/or denaturation under these conditions, even in the presence of EDTA and the enzyme reductase system. The data obtainable down to concentrations of $4 \times 10^{-8}$ M heme (the lower limit in our experience) nevertheless appear to contain a considerable amount of useful information. Their positions and shapes are nearly correct as judged respectively by the constancy of $K_{44}$ values calculated from the median oxygen concentrations, and the comparisons with calculated curves of Figure 8. The development of this new technique by Imai and his colleagues must be regarded as a singular advance of enormous value to the field of hemoglobin research.

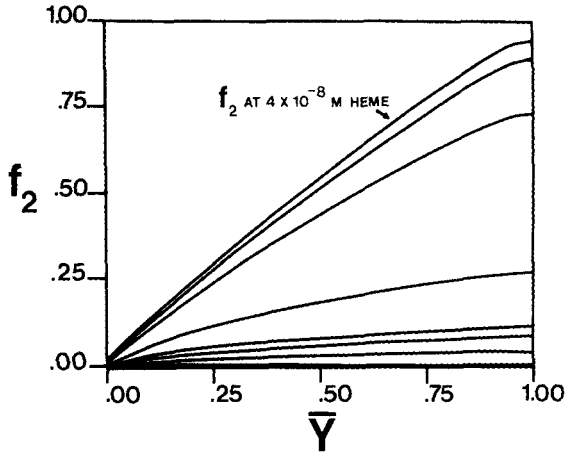


FIGURE 11: Fraction of dimer present in hemoglobin solutions used in this study as a function of hemoglobin oxygenation state.

*The Concentration Dependence of Oxygenation Curves.* The experimental measurements of oxygenation curves as a function of hemoglobin concentration under carefully controlled conditions clearly demonstrate a pronounced concentration dependency effect. The curves are shifted to higher binding affinities with decreasing concentration and also exhibit lowered cooperativity. These results verify previous conclusions regarding the need for caution in analyzing data at a single concentration for the tetramer Adair constants (Ackers et al., 1975). If tetramers alone were present in the hemoglobin samples, no such concentration dependency would exist.

Understanding the source of the observed concentration dependency centers around the question of what molecular species are actually present under conditions of these experiments. We have postulated only dimers and tetramers to be present in appreciable abundance and analyzed the data in terms of the linkage scheme for such a system. The high degree of consistency obtained between the predictions of such a linkage and the experimental data lends credence to this interpretation. In addition, the existence of "clean" reversible equilibria between dimers and tetramers at the two ends of the linkage scheme (i.e., for unliganded and fully oxygenated hemoglobins) is well established by independent studies (Rosemeyer and Huehns, 1967; Chiancone et al., 1968; Anderson et al., 1971; Kellett and Gutfreund, 1970; Kellett and Schachman, 1971; Thomas and Edelstein, 1972; Ip et al., 1976).

There remains the possibility that stoichiometries different from dimer ⇌ tetramer exist under partially oxygenated

conditions. This again seems unlikely in view of the consistency of our results. Preliminary studies on direct measurement of subunit dissociation at partial saturation have been carried out in this laboratory using the equilibrium gel permeation technique with a single-photon counting spectrophotometer (Ackers et al., 1976). The subunit dissociation curve and equilibrium constant obtained at a $pO_2$ of 5 mmHg are in agreement with predictions made from the present analysis of the concentration dependent oxygenation curves. Equilibrium sedimentation studies of partially liganded hemoglobin solutions are also consistent with the dimer–tetramer stoichiometry (Williams, 1976). Further studies of these types will be highly valuable.

Changes in state of oxidation and/or denaturation associated with concentration changes could, in principle, cause changes in shape and position of oxygenation curves. However, it is unlikely that such effects would mimic an oxygenation-linked dimer–tetramer system; nor would they be reversible. Furthermore, these processes have been carefully controlled in the present experiments to levels below that required for appreciable effects of the type described above. Based upon the degree of control over such factors, the independent information on reaction stoichiometries, and the high degree of consistency obtained in our analyses, we believe the dimer–tetramer linkage scheme to be essentially correct.

*Are the Derived Constants Physically Meaningful?* It is possible that, although the linkage scheme is correct, the derived equilibrium constants are computational artifacts, and do not have physical significance. This could arise from a failure to estimate the true values of parameters in the least-squares minimization procedure through, e.g., convergence to a local minimum in residual space. Although such a possibility cannot be totally excluded in any fitting problem of this type, we have taken elaborate precautions against this eventuality by (1) exploring the nature of residual spaces for the fitting problem at hand (see the following paper in this issue), (2) using large numbers of widely varying initial guesses, which yield convergence to the same minimum, (3) fitting to three different sets of parameters from the linkage scheme, which were found to converge to the same solution for the energy distribution.

An additional possibility is that the derived equilibrium constants may be invalid due to systematic errors in the data. For this reason we have eliminated the lowest concentration curves and based our estimates upon the data which is judged on independent grounds to have the highest accuracy and freedom from competing phenomena. These data show essentially random deviations from the best fit to the dimer–tetramer linkage scheme and have a variance which is well within the limits for meaningful solution, based on extensive numerical analyses of the problem (see the following paper). Thus, unless the linkage scheme itself is incorrect, the derived constants are valid to within limits of estimated error.

In sum, we believe these experimental results and analyses, taken together with independently derived information, provide strong verification of the basic linkage relationships postulated to be operative in human hemoglobin under these conditions, and that the derived constants are physically meaningful.

*Resolution of Species Distributions.* The distributions of hemoglobin species derived in this study are shown in Figures 9–11 for isolated tetramers, isolated dimers, and dimers in the complete linked system, respectively. The tetramer distribution (Figure 9) includes only very small amounts of doubly and triply liganded forms, consistent with the high cooperativity under these conditions ($n_{max} = 3.3$) and with the difficulty in estimating the constants $K_{42}$ and $K_{43}$.

The limits of resolution for dimeric species distributions are illustrated in Figure 10. A consequence of the small dimer anticooperativity found in the case A analysis is seen to be an increase in the population of singly liganded dimers, relative to the noncooperative case (case C). Although previous work (Anderson et al., 1971; Kellett, 1971a) has shown dimer cooperativity to be low, the present study is the first one which permits any quantitative estimates to be made on the limits of such cooperativity. Noncooperativity of isolated dimers of course does not imply them to be noncooperative within the tetramer.

The fraction of hemoglobin present as dimers (in all states) is depicted in Figure 11 as a function of hemoglobin concentration. It can be seen that, at the lowest protein concentrations used in this study ($4 \times 10^{-8}$ M), the fraction dimer covers nearly the entire range from zero to unity during the course of oxygenation.

*The Energy States Assumed by Tetrameric Human Hemoglobin.* Based upon the results obtained in this study, there appear to be at least three major energetic states assumed by tetrameric hemoglobin as a function of oxygenation state: (a) unliganded, (b) singly liganded, (c) triply and quadruply liganded species. The energetic partitioning between the second and third binding steps cannot be resolved by present methods into changes at the contact region alone (Ackers and Halvorson, 1974). The average values, which sum to $\delta\Delta G_{13}'$ are listed in Table VI along with the contact energy changes for the first and last steps. It should be noted that $\delta\Delta G_{01}'$ and $\delta\Delta G_{34}'$ are well-defined energy changes for the contact region separating $\alpha^1\beta^1$ dimer pairs within the tetramers. The results provide unequivocal evidence against a concerted transition at a particular binding step in a system with only two energetic states of tetramer (e.g., a "switch" from T to R states at a particular binding step).

We wish to emphasize that the thermodynamic quantities we have determined are entirely independent of molecular models of hemoglobin action but impose constraints that must be met by any model purporting to explain the behavior of human hemoglobin. Results of this study by themselves, however, suggest a fascinating picture of the energy balance between heme binding sites and dimer–dimer contact sites. During the oxygenation–deoxygenation cycle, successive changes in ligand binding energy (i.e., the cooperative energy changes) are accompanied by changes in the intersubunit contact energy which are equal in magnitude but opposite in sign, i.e.

$$\overline{\Delta G_{4m}'} - \Delta G_{41}' = \overline{\delta\Delta G_{13}'} - \delta\Delta G_{01}' \qquad (9)$$

$$\Delta G_{44}' - \overline{G\Delta_{4m}'} = \delta\Delta G_{34}' - \overline{\delta\Delta G_{13}'} \qquad (10)$$

where

$$\overline{\Delta G_{4m}'} = \tfrac{1}{2}(\Delta G_{42}' + \Delta G_{43}')$$

and

$$\overline{\delta\Delta G_{13}'} = \tfrac{1}{2}({}^3\Delta G_2 - {}'\Delta G_2)$$

This principle of complementarity is a consequence of noncooperativity in dimeric species, established in the present studies to be accurate to within approximately ±0.3 kcal/mol of dimer, and strongly suggests that hemoglobin operates at constant energy with respect to these two classes of interactions.

It is not known whether this energy balance is maintained in a single tetrameric molecule or whether it represents an

average over a distribution of more fixed conformational states, with the distribution changing as a function of ligation. The simplest case of the latter principle would correspond to the two-state allosteric model of Monod et al. (1965) in which the T state tetramers are endowed with a small negative free energy of oxygen binding but large negative free energy of subunit interaction, and the R state tetramers have higher binding energies and lower subunit interaction energies. We have tested our experimentally derived energies for consistency with the MWC (Monod-Wyman-Changeux) model and found them to be in reasonable agreement. It should be noted, however, that such agreement does not provide direct evidence in favor of a model; in principle the set of energies we have determined constitutes information capable of excluding such models. Clearly a wider range of conditions (temperature, pH, etc.) needs to be explored in this regard.

*Future Prospects.* It is interesting to note that one of the earliest theories of hemoglobin cooperativity (Douglas et al., 1912) was based upon the notion that unliganded hemoglobin is more aggregated than oxyhemoglobin (cf. Edsall, 1972). Although the oxygenation-linked association-dissociation equilibria of human hemoglobin are not of physiological significance per se, their study does provide a powerful means to probe the intersubunit contact energy changes which accompany cooperative ligand binding. The present work represents the first detailed experimental study using this approach.

Numerical values reported here pertain only to one particular set of conditions and the explicit results may be of less importance than the fact that we have now generated the capability of solving this energy distribution problem in a variety of hemoglobins. Extensions of the approach we have developed may fruitfully proceed in several directions: to include mutant and chemically modified hemoglobins, and to encompass a wider range of conditions (temperature, pH, ionic strength, effectors, etc.). Knowledge of the contact energy changes in a variety of hemoglobins, having structural differences within the contact region, may permit a more detailed mechanistic understanding of the specific interactions responsible for constraints within this region, their individual energies, the sequence of their release during oxygenation, and their control by specific effectors and environmental conditions.

## Acknowledgments

We are grateful to Drs. K. Imai (Osaka University) and T. Yonetani (University of Pennsylvania) for valuable information on construction and operation of the automatic oxygenation apparatus. Preparation and characterization of the isolated hemoglobin chains used in this study were carried out by Dr. Roland Valdes. This work has benefited greatly from critical discussions with Drs. J. T. Edsall, R. C. Williams, Jr., H. R. Halvorson, R. P. Taylor, and R. L. Biltonen. We also thank the University of Virginia Computing Center for enormous amounts of time on the CDC 6400 computer.

## Appendix

*Definition of Parameters in the Saturation Function.* The saturation linkage function, eq 1, is defined in terms of the following polynomials:

$$Z_2 = 1 + K_{21}[X] + K_{22}[X]^2$$

$$Z_2' = K_{21} + 2K_{22}[X]$$

$$Z_4 = 1 + K_{41}[X] + K_{42}[X]^2 + K_{43}[X]^3 + K_{44}[X]^4$$

$$Z_4' = K_{41} + 2K_{42}[X] + 3K_{43}[X]^2 + 4K_{44}[X]^3$$

where

$$K_{ni} = \frac{[(\alpha_{n/2}\beta_{n/2})[X_i]]}{[(\alpha_{n/2}\beta_{n/2})][X]^i} \quad \begin{matrix} n = 2, 4 \\ i = 1, 2, 3, 4 \end{matrix}$$

For more extensive definitions of the equilibrium constants and the relationships between them, the reader is referred to: Ackers and Halvorson, 1974; Johnson et al., 1976.

*The Wyman Interaction Energy for a Dimer-Tetramer System.* The function $\bar{Y}/(1 - \bar{Y})$ for a linked dimer-tetramer system can be calculated from the saturation eq 1. The limiting forms of this function as ligand concentrations [X] approaches zero and infinity are given by eq 5 and 6. The function $\bar{Y}/(1 - \bar{Y})$ reduces to the following limiting forms in terms of protein concentration.

(1) At infinitely low protein concentration, where only dimers would exist

$$\lim_{[P_t]\to 0} \left(\frac{\bar{Y}}{1-\bar{Y}}\right)_{[X]\to 0} = \frac{1}{2}K_{21}[X]$$

$$\lim_{[P_t]\to 0} \left(\frac{\bar{Y}}{1-\bar{Y}}\right)_{[X]\to \infty} = 2\frac{K_{22}[X]}{K_{21}}$$

The Wyman interaction energy $\Delta G_1$ corresponding to these limits is then

$$\Delta G_1(0) = RT \ln \left(\frac{K_{22}}{K_{21}^2}\right)$$

(2) At the limit of infinitely high protein concentration, only tetramers would exist and

$$\lim_{[P_t]\to \infty} \left(\frac{\bar{Y}}{1-\bar{Y}}\right)_{[X]\to 0} = \frac{1}{4}K_{41}[X]$$

$$\lim_{[P_t]\to \infty} \left(\frac{\bar{Y}}{1-\bar{Y}}\right)_{[X]\to \infty} = \frac{4K_{44}}{K_{43}[X]}$$

The Wyman interaction energy then becomes

$$\Delta G(\infty) = RT \ln \left(\frac{16K_{44}}{K_{43}K_{41}}\right)$$

The quantities $\Delta G_1(0)$ and $\Delta G_1(\infty)$ are equal to the differences in free energies of binding (corrected for statistical factors) in the last and first steps for dimer and tetramer, respectively (Saroff and Minton, 1972).

## References

Ackers, G. K. (1975), *Proteins, 3rd Ed. 1,* 1-94.

Ackers, G. K., Brumbaugh, E. E., Ip, S. H. C., and Halvorson, H. R. (1976b), *Biophys. Chem. 4,* 171-179.

Ackers, G. K., and Halvorson, H. R. (1974), *Proc. Natl. Acad. Sci. U.S.A. 71,* 4312-4316.

Ackers, G. K., Johnson, M. L., Mills, F. C., Halvorson, H. R., and Shapiro, S. (1975), *Biochemistry 14,* 5128-5134.

Ackers, G. K., Johnson, M. L., Mills, F. C., and Ip, S. H. C. (1976a), *Biochem. Biophys. Res. Commun. 69,* 135-142.

Ames, B. N., and Dubin, D. T. (1960), *J. Biol. Chem. 235,* 769-775.

Anderson, M. E., Moffat, J. K., and Gibson, Q. H. (1971), *J. Biol. Chem. 246,* 2796-2807.

Benesch, R. E., Benesch, R., and Yung, S. (1973), *Anal. Biochem. 55,* 245-248.

Brunori, M., Noble, R. W., Antonini, E., and Wyman, Jr. (1966), *J. Biol. Chem. 241,* 5238-5243.

Bucci, E., and Fronticelli, C. (1965), *J. Mol. Biol. 12,* 183-192.

Chiancone, E., Gilbert, L. M., Gilbert, G. A., and Kellett, G.

L. (1968), *J. Biol. Chem. 243,* 1212–1219.
Douglas, C. G., Haldane, J. S., and Haldane, J. B. S. (1912), *J. Physiol. 44,* 275–304.
Edsall, J. T. (1972), *J. Hist. Biol. 5,* 205–257.
Haupt, G. W. (1952), *J. Opt. Soc Am. 42,* 441–447.
Hayashi, A., Suzuki, T., and Shin, M. (1973), *Biochem. Biophys. Acta 310,* 309–316.
Hewitt, J. A., Kilmartin, J. V., Ten Eyck, L. F., and Perutz, M. F. (1972), *Proc. Natl. Acad. Sci. U.S.A. 69,* 203–207.
Imai, K. (1973), *Biochemistry 12,* 798–808.
Imai, K., Morimoto, H., Kotani, M., Watari, H., Waka, H., and Kuroda, M. (1970), *Biochim. Biophys. Acta 200,* 189–196.
Ip, S. H. C., Johnson, M. L., and Ackers, G. K. (1976), *Biochemistry 15,* 654–660.
Johnson, M. L., Halvorson, H. R., and Ackers, G. K. (1976), *Biochemistry,* the following paper in this issue.
Kellett, G. L. (1971a), *Nature (London) 234,* 189–191.
Kellett, G. L. (1971b), *J. Mol. Biol. 59,* 401–424.
Kellett, G. L., and Gutfreund, H. (1970), *Nature (London) 227,* 921–926.
Kellett, G. L., and Schachman, H. K. (1971), *J. Mol. Biol. 59,* 387–399.
Lumry, R. (1971), in Electron and Coupled Energy Transfer in Biological Systems, Vol. I, Part A, King, T. P., and Klingenberg, G., Ed., New York, N.Y., Marcel Dekker, pp 1–108.
Monod, J., Wyman, J., and Changeux, (1965), *J. Mol. Biol. 12,* 88–118.
Perutz, M. F. (1970), *Nature (London) 228,* 726–734.
Perutz, M. F., and Ten Eyck, L. F. (1971), *Cold Spring Harbor Symp. Quant. Biol. 36,* 295–370.
Rifkind, J. (1974), *Biochemistry 13,* 2475–2481.
Rosemeyer, M. A., and Huehns, E. R. (1967), *J. Mol. Biol. 25,* 253–273.
Saroff, H. A., and Minton, A. P. (1972), *Science 175,* 1253–1255.
Shimizu, K., and Bucci, E. (1974), *Biochemistry 13,* 809–814.
Soni, S. K. (1973), Ph.D. Thesis, University of Tennessee.
Thomas, J. O., and Edelstein, S. J. (1972), *J. Biol. Chem. 247,* 7870–7874.
Thomas, J. O., and Edelstein, S. J. (1973), *J. Biol. Chem. 249,* 2901–2905.
Tyuma, I., Benesch, R. E., and Benesch, R. (1966), *Biochemistry 5,* 2957–2962.
Weber, G. (1975), *Adv. Protein Chem. 29,* 1–83.
Williams, R. C., Jr. (1976), Abstracts, 20th Annual Meeting of the Biophysical Society, Seattle, Washington.
Williams, R. C., Jr., and Tsay, K. (1973), *Anal. Biochem. 54,* 137–145.
Winterhalter, K., and Colosimo, A. (1971), *Biochemistry 10,* 621–623.
Wyman, J. (1964), *Adv. Protein Chem. 19,* 223–289.